(NASA-CR-194169) CONTINUED DEVELOPMENT OF AN ULTRA-NARROW BANDPASS FILTER FOR SOLAR RESEARCH Final Technical Report (JHU) 17 p

N94-10735

Unclas

G3/74 0183091

The Johns Hopkins University

Applied Physics Laboratory

Final Technical Report

NASA Task 170-38-51-02-10, "Continued Development of an Ultra-Narrow Bandpass Filter for Solar Research"

Grant: NAGW-2416

P. I.: Dr. David M. Rust

Report Date: September 9, 1993

The objective of work under this task was to develop ultra-narrow optical bandpass filters and related technology necessary for construction of a compact solar telescope capable of operating unattended in space. The scientific problems to which such a telescope could be applied include solar seismology, solar activity monitoring, solar irradiance variations, solar magnetic field evolution, and the location of targets for narrow-field specialized telescopes.

We designed a Y-cut lithium-niobate Fabry-Perot etalon and had it fabricated and tested. It was examined with a dye laser at our laboratories and with sunlight at the National Solar Observatory. We found that the Y-cut etalon has 2.5 X greater response to applied voltage than the Z-cut etalons made under earlier grants. This makes the filter much more flexible and makes possible a 'universal' filter for the 3500 - 7000 Å spectral range. The etalon will be used in the up-coming Flare Genesis Experiment.

Work performed under the grant validated our design of a versatile solar telescope. It will be flown on a stratospheric balloon rather than on a spacecraft, because of the curtailed launch opportunities. In applying the filter in the Flare Genesis Experiment, we have gone well beyond the grant objective to develop a filter for a compact telescope. The filters developed under this grant and the previous NASA grant will be used with one of the largest solar telescopes in the world. The Flare Genesis Experiment will investigate solar magnetic fields, but it can also study solar seismology, solar irradiance variations, and other important research problems, thanks to the relatively-economical F-P etalons.

One specific objective of the work performed under this task was to improve the auxiliary filters, called blockers, that are necessary to make effective use of tunable Fabry-Perot etalons and other bandpass filters with a restricted free spectral range. Toward this objective, we designed a tunable liquid-crystal Fabry-Perot filter with a 50-mm aperture. The filter was fabricated by Meadowlark Optics, Inc., and we tested it at the National Solar Observatory. The filter performed well, but its passband was about twice the specified passband, so it was returned for reworking. Achieving our specification has proved to be a very difficult task, but the contractor expects to ship a functional filter by the end of the year.

We have discussed the problem of finding suitable blockers with CSIRO (Sydney, Australia). They believe they can make a double-cavity Fabry-Perot etalon that will be tunable over the entire visible spectrum and will require only 50-Å blockers, which are commercially available. We also tested a tunable Lyot-type filter, made by Cambridge Research Instruments, Inc. Their filter showed promise as a blocker for our etalons, but it lacked the temperature control necessary for reliable operation. Since then, CRI has marketed a tunable blocker similar to the one tested at our facilties. Thus, our work with their filters under the NASA grant has spurred some deeper thinking by suppliers and seems likely to lead to a 'universal' narrow-band optical filter in the near future.

Another objective under the subject grant was to design and test a breadboard model of a telescope that can form images of the full sun when used with an ultra-narrow bandpass filter. Under the subject grant, we completed the telescope design. Under another grant, we built a 100-mm aperture telescope for full-disk imaging. This telescope will be the target selector for the Flare Genesis Experiment. It is in the final stages of test now. This compact telescope represents a significant improvement over present designs because it achieves simultaneous high spatial and high spectral resolution over the full sun. Until recently, magnetographs have had to scan or image only a small fraction of the solar disk at a time. With a suitably blocked lithium niobate etalon filter, the entire solar disk can be sampled at once in the wing of a magnetically sensitive spectral line.

Other work performed under the subject grant included modification of the APL Solar Observatory to allow mounting test optics near the focus of the 15-cm telescope. We can now easily test optical breadboard systems. Two new benches were installed for optical rails on which we can mount CCD cameras and a spectrograph. A summer student used the equipment to test blocker filters for the etalons. It was also used to test CRI blockers.

In summary, we have demonstrated an easily-tuned filter of Y-cut lithium niobate. This filter will be used on the Flare Genesis Experiment. We also obtained solar images with a Z-cut etalon. We believe that work under this grant will lead to the commercial availability of a universal optical filter with approximately 0.1 Å bandwidth. Progress was made toward making a suitable 1 - 2 Å tunable blocker filter, but it now appears that the best approach is to make a double-cavity etalon that will not require such a narrow blocker. Broader band blockers are commercially available.

<u>Relevant Publications</u>

Burton, C. H., Leistner, A. J., and Rust, D. M., 1987, "Electrooptic Fabry-Perot Filter: Development for the Study of Solar Oscillations," *Applied Optics* **26**, 2637.

Rust, D. M. and Appourchaux, T., 1988, "The Stable Solar Analyzer," *Proc. Symp. Seismology of the Sun and Sun-like Stars,"* European Space Agency, ESA SP-286, p. 227.

Rust, D. M., O'Byrne, J. W., and Harris, T., 1988, "An Optical Instrument for Measuring Solar Magnetism," *Johns Hopkins APL Tech. Dig.* **9**, 349.

Rust, D. M. and O'Byrne, J. W., 1991, "Vector Magnetography," in *Solar Polarimetry* (L. November, ed.), National Solar Observatory, Sunspot, New Mexico, p. 74.

Rust, D. M., 1991, "Etalon Filters," LEST Foundation Tech. Report No. 50, Inst. of Theoretical Astrophys., Univ. of Oslo.

Rust, D. M., 1993, "The Flare Genesis Project," *Adv. Space Res.* (in press).

TECHNICAL REPORT NO. 50

Etalon Filters

David M. Rust

The Johns Hopkins University
Applied Physics Laboratory
Laurel, Maryland 20723

1991

The Technical Report Series is published at
Institute of Theoretical Astrophysics,
University of Oslo

Editors : O. Engvold and Ø. Hauge
Editorial assistants :
L. Gunzinger
K. Strand

ISSN 0800-7780

Contribution to the Workshop on Focal Plane Instrumentation for LEST (Large Earth-based Solar Telescope), Huntsville, Alabama, April 8, 1991.

ETALON FILTERS

David M. Rust
The Johns Hopkins University Applied Physics Laboratory
Laurel, Maryland 20723

Summary

This article begins with a brief introduction to Fabry-Perot interferometers and goes on to describe the use of Fabry-Perot etalons as narrow-band filters. Properties of solid etalons with fused silica, mica and lithium niobate substrates are discussed and compared with those of the familiar Lyot birefringent filter. Examples of applications of etalon filters in helioseismology, high-resolution imaging and vector magnetography are given. It is concluded that lithium niobate etalons can meet the LEST requirements for a universally tunable narrow-band filter.

Fundamentals

"Etalon" means "a standard" by which others can be measured. The kind of etalon discussed in this article was invented by Charles Fabry and Alfred Perot (1898), and it consists of two partially reflective surfaces separated by a narrow cavity. As shown in Figure 1, light transmitted by the first surface may be reflected or transmitted by the second surface. The reflected and transmitted rays combine constructively when the number of waves in the cavity is an integer. Then, light is transmitted by the device according to the Airy formula:

$$I(\delta) = \frac{I(0)}{1 + \frac{4R}{(1-R)^2} sin^2\left(\frac{\delta}{2}\right)}, \quad \text{with } \delta = \frac{2\pi}{\lambda} 2nd \cos\theta \qquad (1)$$

where R is the reflectivity of the surfaces (usually > 0.9), d is the depth of the cavity, n is the index of refraction inside the cavity, λ is the wavelength, and θ is the angle between the rays and the normal to the reflective faces. The equation shows that an etalon can be used as a wavelength standard.

Solar physicists familiar with the Lyot birefringent filter will appreciate a series representation of the Airy formula given in the monograph by Vaughan (1989). Figure 2 shows that the Fabry-Perot transmission pattern is the sum of an infinite number of fringe patterns, just as in the Lyot. In this case, the first term represents the proportion of light transmitted by the two surfaces on the first pass, and there are no fringes. The second term is the low-contrast Michelson fringe pattern produced by a single reflection (one order of interference). With each succeeding reflection, there is less light and the amplitude of the fringes is less, but the order of interference is higher. All the fringes add up to 100% transmission whenever $m\lambda = 2nd \cos\theta$, assuming no losses in the cavity. The quality of an etalon is measured by the finesse $\mathcal{F} = FSR/\Delta\lambda = \lambda^2/2nd$, where the *free spectral range FSR* is the spacing between passbands and $\Delta\lambda$ is the full passband width at half maximum (FWHM).

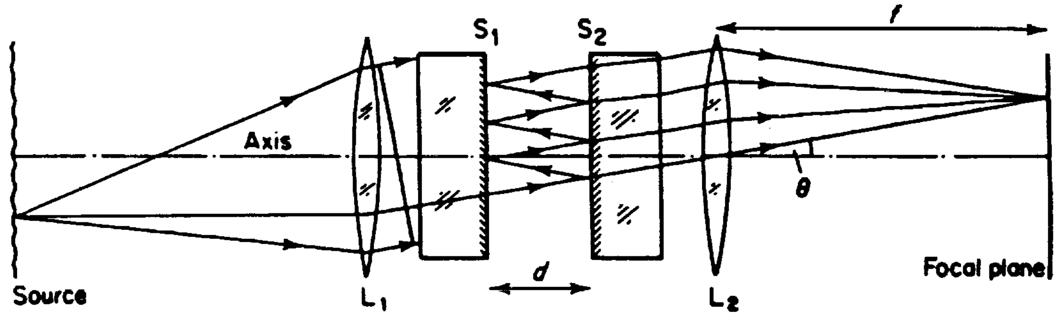

Figure 1. A basic Fabry-Perot Interferometer. S_1 and S_2 are plane parallel, partially-reflecting optical surfaces. L_1 collimates the light from each point in the source. Successively reflected waves are superposed by L_2 to form fringes in the focal plane.

Filters

A Fabry-Perot etalon makes a useful filter when *FSR* is large compared with $\Delta\lambda$, as in the Lyot. Figure 3 compares the theoretical, normalized profiles of Fabry-Perot etalon filters and a nine-element Lyot filter. The single-etalon profile falls off slower than the Lyot profile, but two etalons in series will give a contrast comparable to that attainable with the Lyot. The FWHM of two similar etalons in series is 62 % of the width of a single etalon. Figure 3 shows the transmission profile of a double etalon, *i.e.*, two etalons optically contacted so that interference is obtained in three cavities: the two narrow ones and the doubly-thick one.

Air spaced etalons are frequently used in astronomy, and they have the advantage that the spacing between the faces can be varied. Bray (1988) proposed a three-stage, air-spaced etalon filter for the LEST. In his filter, each etalon blocks the unwanted passbands of the others. The resultant filter is a fully tunable or 'universal' filter, but the air-spaced etalons require sophisticated control schemes to maintain the parallelism of the faces and to compensate for air pressure and temperature changes.

The filters emphasized in this article are all solid etalons, that is, the reflecting surfaces are deposited on the highly polished and parallel faces of a transparent substrate of index *n*. Making solid etalons is a technical challenge because the faces must be flat and parallel to ~ $\lambda/100$, but maintaining parallelism is not a problem after fabrication. Several manufacturers offer excellent etalons with apertures as large as 75 mm. The finesse is usually 20 - 60, so intermediate blockers are necessary for solar work, where $\Delta\lambda$ = 0.05 - 1.0 Å. A broad-band filter or another etalon will block unwanted transmission bands.

Tuning

Equation (1) reveals that the wavelengths of the passbands depend on the incident angle of the beam. The tuning effect in a fused silica etalon is shown in Figure 4a. Tilting an etalon always broadens the passband and shifts it to the blue: $\delta\lambda = -\lambda^2/2n^2$. Tilts of greater than 2° generally produce unacceptable broadening.

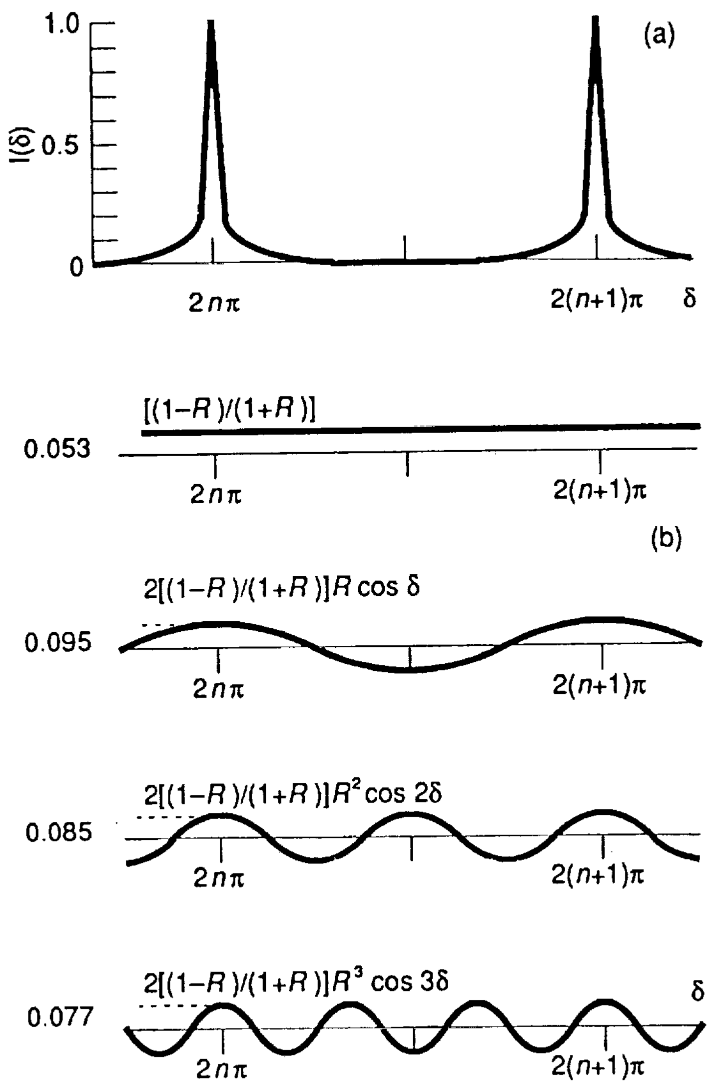

Figure 2. (a) The Airy distribution (equation (1)) with R = 0.9. (b) The first four terms of the equivalent series expansion (from Vaughan, 1989).

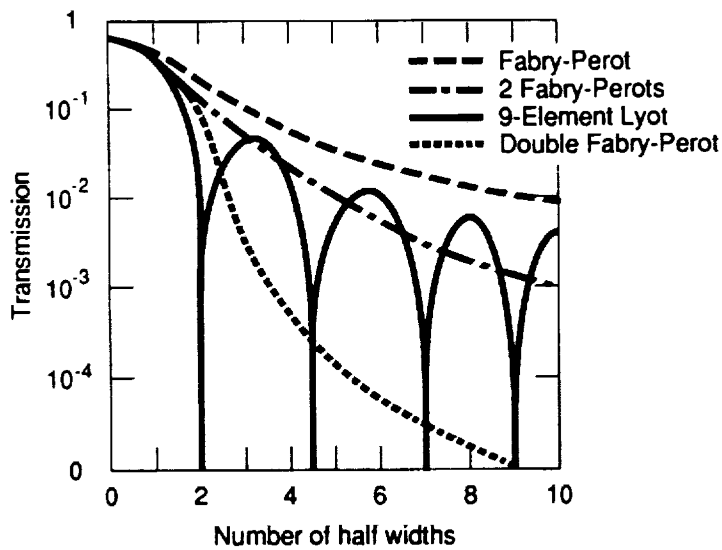

Figure 3. Etalon filter profiles compared with the profile of a nine-element birefringent filter (from Austin, 1972).

Figure 4b shows the effect of beam convergence. Note the passband broadening and the drop in peak transmission for beams faster than F/30. This effect is not as serious in high-index materials as in air-spaced etalons, because of the n^{-2} dependence of $\delta\lambda$.

Nature provides acceptable etalon substrates in the form of mica sheets, for which n_e = 1.596 and n_o = 1.591. Because mica has two indices of refraction, two sets of passbands are formed. A rotating polarizer in the beam will tune from one set to the other. Smartt (1982) exploited this effect with a photometer that chops rapidly between the coronal green line and the nearby continuum so that fluctuations in sky transparency could be removed. Mica etalon filters are relatively inexpensive, but they cannot practically be made narrower than 0.5 Å, and absorption will usually limit the transmission to < 30 %.

Solid etalon filters may be tuned by changing the temperature. A mica filter will shift redward by ~ 1 Å, or about *FSR/20*, for each 16° C increase in temperature, and a lithium niobate ($LiNbO_3$) filter (Rust *et al.*, 1986) will shift by ~ 0.5 Å, or *FSR/7* for the same temperature increase. It is obvious from this that a universal temperature-tuned filter would be impractical since shifts of ±*FSR/2* are required to reach all wavelengths.

The refractive index of lithium niobate (n = 2.23) changes slightly upon application of an electric field. Thus, voltage applied across a conductive layer deposited on the etalon faces will change the optical length of the resonant cavity and allow passband tuning. The tuning constant is 0.4 mÅ/volt or ±*FSR/2* per ±4000 V in the etalon used in the JHU/APL vector magnetograph (Rust and O'Byrne, 1991). This etalon has a bandwidth of 167 mÅ and a peak transmission of

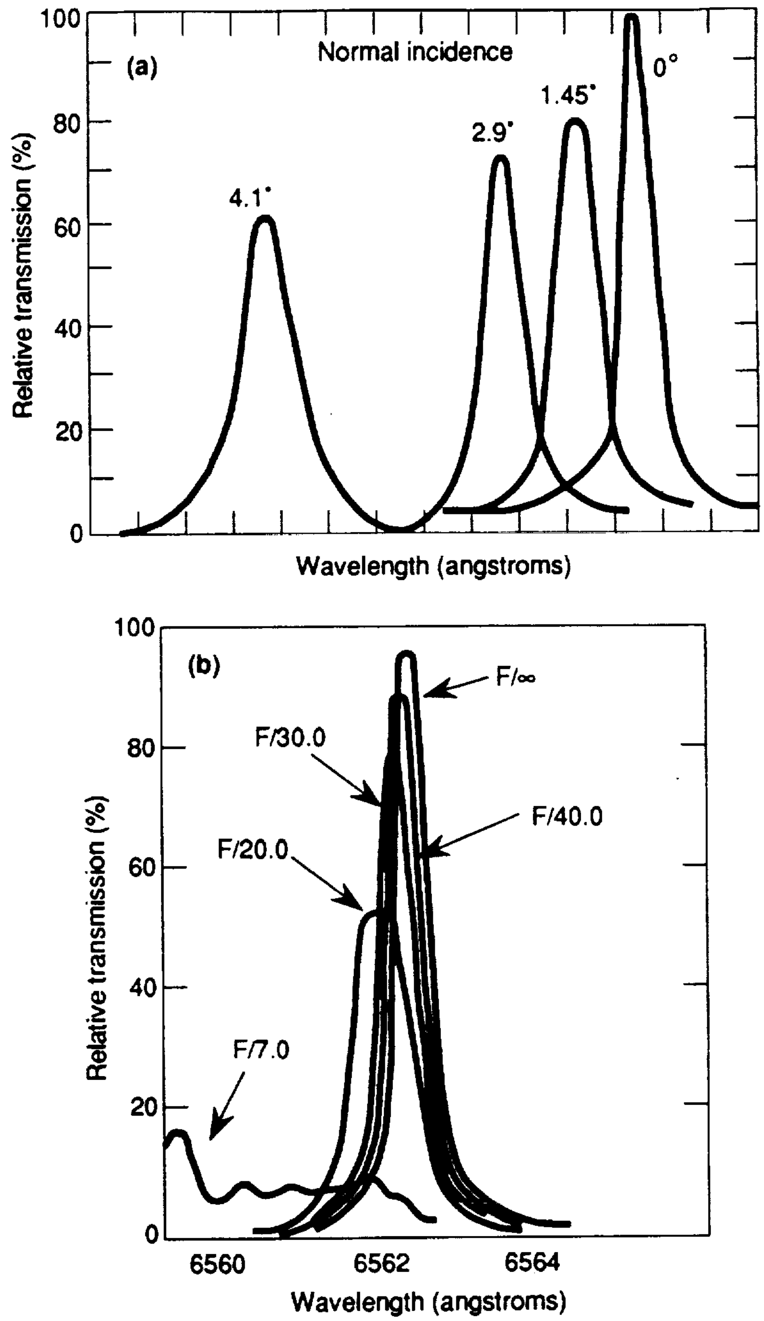

Figure 4. (a) Relative transmission of a fused silica etalon at varying degrees of tilt in a collimated beam. (b) Relative transmission of the etalon in convergent beams (from Austin, 1972).

50%. The etalon is made from a 75-mm diameter wafer of crystalline, Z-cut lithium niobate polished to a thickness of 220 μm and 1/400th-wave rms flatness. The finesse is 21, and the contrast between transmission at the peak and at the minima between peaks is 180. The dielectric coatings on the surfaces are 93% reflecting over a 6000 - 8000 Å band, and they determine the operating range of the filter. Lithium niobate is transparent from 0.4 μm, so two or three etalons with different dielectric coatings would cover the visible spectrum. In the infrared, gold can double as both reflective coating and conductor, so a single etalon will serve from 1 μm to ~ 4 μm, where lithium niobate becomes opaque.

Commercial applications for lithium niobate that have nothing to do with optical filters have fueled dramatic improvements in this man-made crystal. At least one company is now offering exceptionally uniform and pure 100-mm diameter wafers. The CSIRO National Measurement Laboratory in Sydney, Australia, where our etalons were made, has not made an etalon from this new material yet, but I expect that the recent improvements will increase the peak transmission above the 50 % achieved with the old material and raise the finesse from 20 - 25 to ~40.

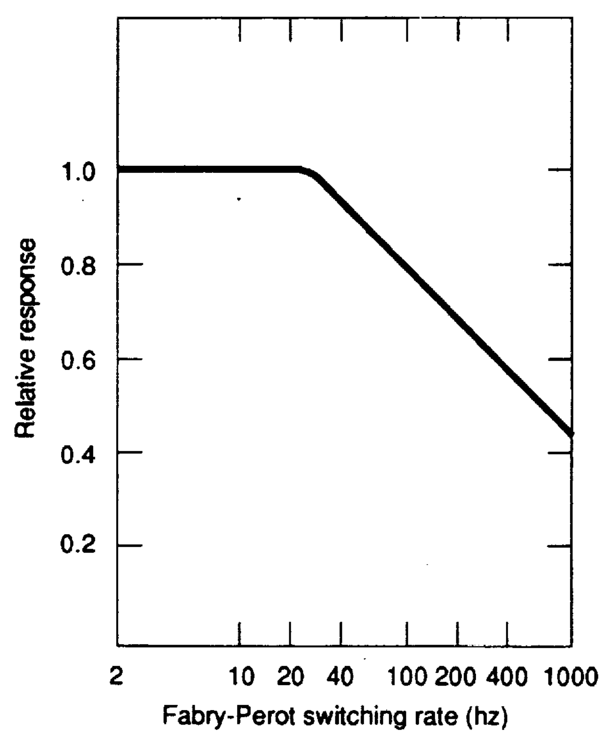

Figure 5. Relative sensitivity to a 30-mÅ Doppler shift of an instrument using a lithium niobate etalon subjected to an impressed square-wave voltage of 400-V p-p.

Tuning speed is an important issue in some applications, *e.g.*, in helioseismology. Figure 5 shows the results of a test at the Mount Wilson Observatory where a lithium niobate etalon was tuned with a 400 V (= 0.16 Å) square-wave signal. The effect in the transmitted solar light was to chop from wing to wing of the Ca I line at 6122 Å. When the mean passband was offset slightly from line center, an alternating signal was developed. This signal was detected with a silicon diode and then rectified with a phase-sensitive amplifier. The results are plotted in Figure 5. The figure shows that the signal amplitude was undiminished until ~ 30 Hz. It then dropped as one would predict from the 2.5 nanofarad filter capacitance, but the relative Doppler signal sensitivity was still 0.5 at 600 Hz. The test shows that a lithium niobate filter can be tuned at video rates with no loss of signal.

A Z-cut $LiNbO_3$ crystal has only one index of refraction for on-axis rays, but a Y-cut crystal has two indices of refraction, one of them much more sensitive to voltage than the other. Bonaccini and Smartt (1988) pointed out that an etalon filter could be made from Y-cut lithium niobate to give two sets of passbands. Figure 6 shows how a passband corresponding to the ordinary rays can be shifted by 1 Å while that for the extraordinary ray is stable to within ~ 0.04 Å. This capability should prove useful in coronal-line profiling and in the infrared, particularly for the Helium line at 10830 Å, where light from the underlying photosphere must always be subtracted.

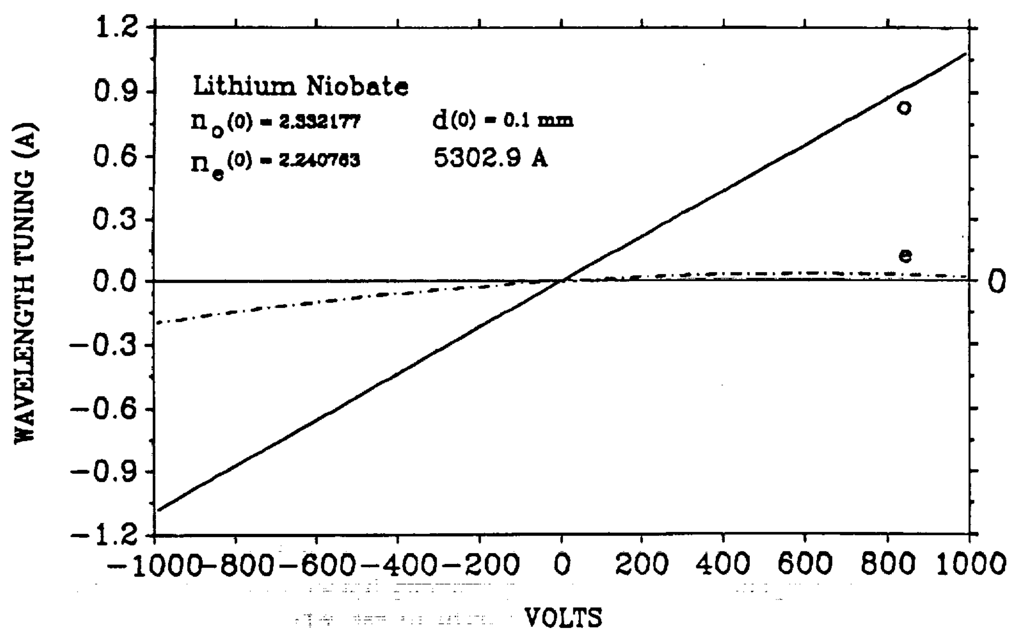

Figure 6. Voltage sensitivity of the passbands of a Y-cut lithium niobate etalon (from Bonaccini and Smartt, 1988).

Stability

An important requirement in most filter applications is wavelength stability. Air-spaced etalons must be housed in temperature-controlled, hermetically-sealed chambers to avoid wavelength shifts. Solid etalons are sensitive only to temperature changes. They are inherently easier to stabilize. Temperature control to ±0.1° C is usually sufficient to maintain ±5 mÅ wavelength stability. If higher stability is required, a lithium niobate etalon can be monitored with a stabilized laser and controlled with a servo circuit. One etalon was stabilized to one part in 10^{10} (= 5 cm s^{-1} Doppler signal) against passband shifts that could mimic 5-min solar oscillations (Rust, Appourchaux and Hill, 1988).

Experience with etalon filters

A fused silica etalon (Austin, 1972) aboard the Skylab Apollo Telescope Mount provided H_α filtergrams for comparison of chromospheric structures with the X-ray and UV structures seen with the other Skylab telescopes. Mica etalons marketed by the Daystar Corporation are used at hundreds of observatories around the world, including the APL vector magnetograph at Sacramento Peak, where one is used to block the unwanted orders of a lithium niobate filter. Figure 7 is an H_α filtergram obtained with these filter during a field trip to the Big Bear Solar Observatory. The image quality is excellent, as it usually is at Big Bear, but the picture is so good that I wondered if etalon filtergrams could routinely be superior to Lyot filtergrams. Figure 8 shows a comparison of video magnetograms made with an etalon filter and with a Lyot. The new magnetogram looks better. We plan further comparisons, but there *should* be less image distortion in a 0.2-mm thick wafer than in ~ 20 elements (= 25 cm) of calcite and quartz.

The most demanding application of a lithium niobate etalon to date has been in the APL vector magnetograph (Rust and O'Byrne, 1991). In this instrument, the beam from a 4-arcmin field is expanded to take full advantage of the 65-mm aperture of the etalon. The larger aperture allows narrower cone angles and thus higher spectral resolution (ref. Figure 4b). Figure 9 is a vector magnetogram obtained with the etalon filter tuned to the blue wing of the Ca I line at 6122 Å. The magnetic field values have been corrected everywhere for the effects of the slope of the line; that is, the etalon was tuned to simulate a Zeeman shift and then the real signals were compared with this calibration signal, pixel-by-pixel. Both signals are proportional to the slope, so local variations in slope cancel out. The filter was tuned automatically during the observations so that the calibration signal was developed simultaneously with the actual measurements.

Application to LEST

The resolving power, $\mathcal{R} = \lambda/\Delta\lambda$, of the existing lithium niobate etalons is 36000, which is appropriate for vector magnetography and filtergrammetry but too low for Stokes polarimetry. For that, $\mathcal{R}$ = 100000 is more appropriate, so we need to ask whether an etalon filter with this resolving power can accept a beam from a LEST-sized field. Figure 10 is a graphical representation of the relevant throughput/spectral-resolution relation: $\Omega x \mathcal{R} = 2\pi n^2$, where Ω is the effective solid angle at the filter of the field of view. The graph is drawn for n = 1, and to get the angular diameter ψ of the field that can be imaged at resolution $\mathcal{R}$, we must multiply the numbers on the abcissa by n.

Figure 7. Solar active region NOAA 6063 recorded at the Big Bear Solar Observatory on 17 May 1990 with a 167-mÅ lithium niobate etalon tuned to H_α line center.

Figure 8. (a) A longitudinal magnetogram obtained at 6122 Å on 15 October 1990, during a test of a lithium niobate etalon at the Big Bear Solar Observatory.

Figure 8. (b) A longitudinal magnetogram obtained at 6103 Å on 15 October 1990, seven minutes before the magnetogram in Figure 8(a). This magnetogram was made with the Zeiss birefringent filter at Big Bear.

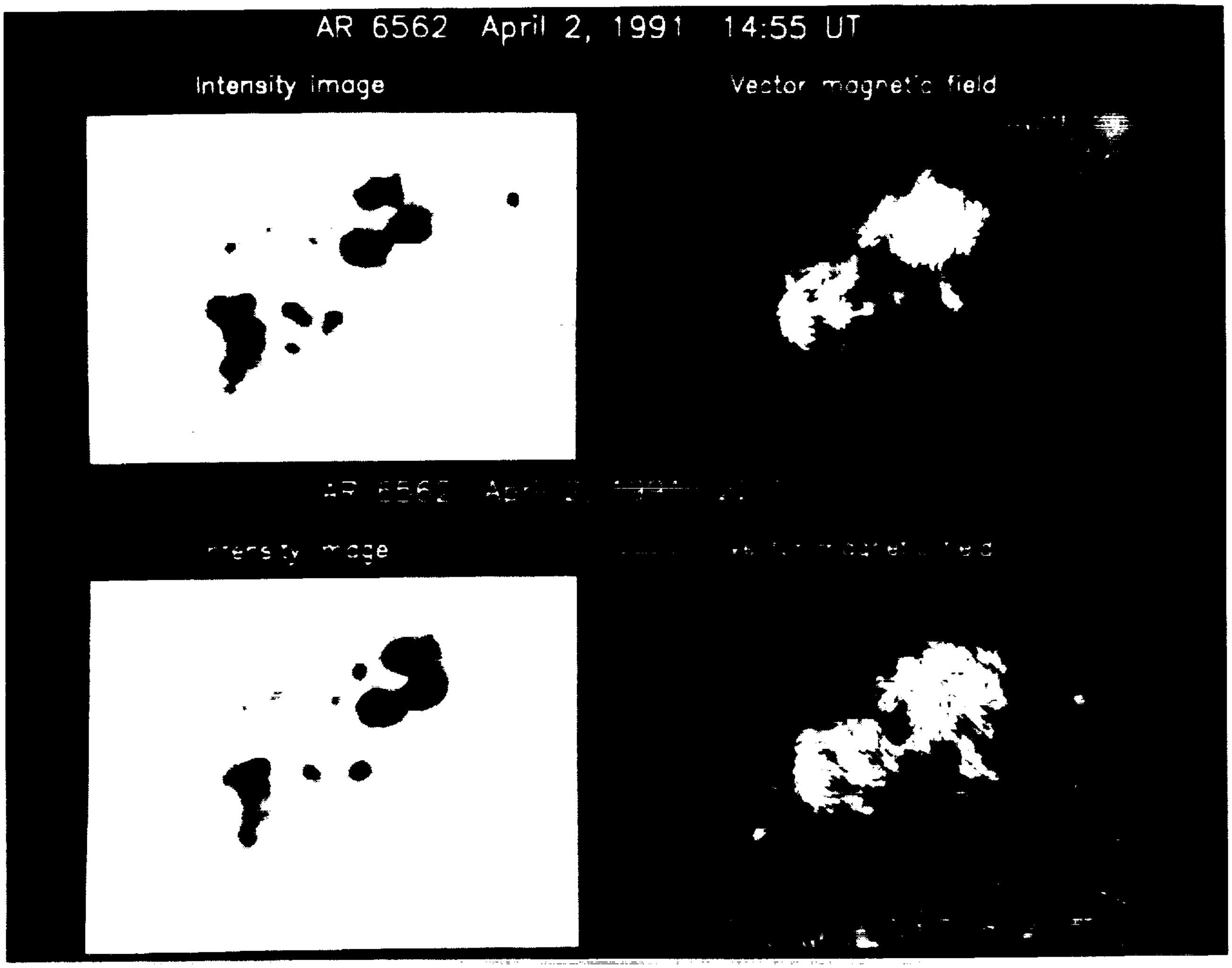

Figure 9. Vector magnetograms obtained at the Sacramento Peak Observatory on 2 April 1991 with the APL magnetograph tuned to 6122 Å.

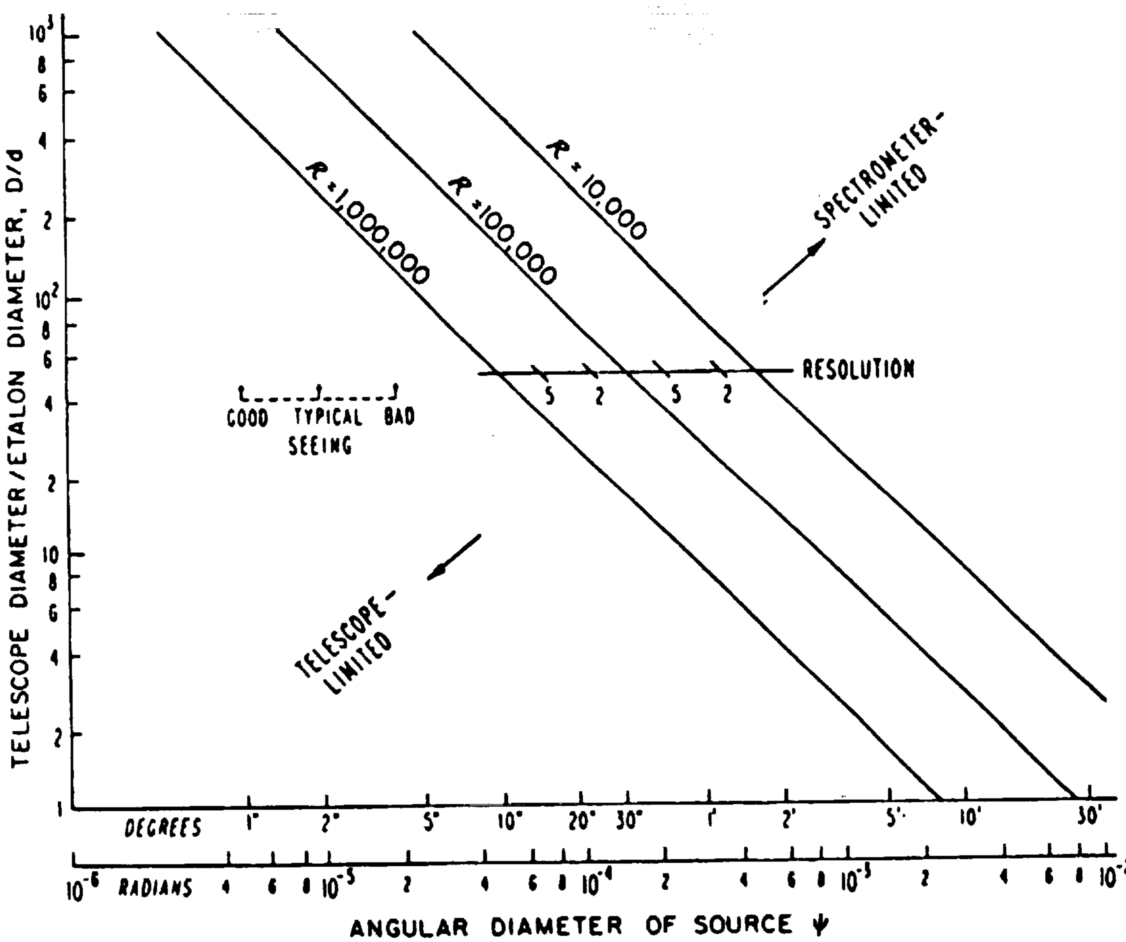

Figure 10. The ratio of telescope diameter to etalon diameter required for various spectral resolutions. The angular diameter of the field of view that can be studied at resolution R with an air-spaced etalon is given on the abscissa. Use of a solid etalon increases the field of view by the refractive index n.

The LEST aperture is 2.4 m, and the largest etalon that can be made today would have a clear aperture of 95 mm. With a ratio of diameters of ~ 25, an air-spaced etalon can operate at $\mathcal{R}$ = 100000 over a 1' field of view. This translates into a 2.23' field of view for a lithium niobate etalon.

Conclusion

Lithium niobate etalons have emerged as valuable tools in solar physics. They can be used at the LEST for high-resolution imaging and helioseismology. Stokes polarimetry and other applications requiring a spectral resolution of 100000 would call for two 95-mm etalons in series, each with *FSR* ~ 3.2 Å, the same as for our present etalons. The *FSR* of one etalon should differ from the other by ~10 % so that the effective *FSR* of the pair is ~ 32 Å. At a finesse of 40, $\Delta\lambda$ = 0.08 Å for each etalon, but together they give $\Delta\lambda$ = 0.05 Å. Unwanted orders can be blocked with commercial 50-Å thin-film filters. A set of these will allow use of the etalons at all wavelengths permitted by their reflective coatings. With several pairs of etalons, the entire spectral range from 0.4 μm to 4.0 μm can be studied at $\mathcal{R}$ = 100000.

Acknowledgments

I am grateful to the CSIRO National Measurement Laboratory and to the Daystar Corporation for providing many excellent filters, and I thank Sara Martin and the staff of the Big Bear Solar Observatory for their support of my observations there. This work was supported by the JHU/APL Independent Research and Development Program and by grants AFOSR-87-0077, AFOSR-90-0102, and NAGW-2416 (NASA).

References

Austin, R. R., 1972, The use of solid etalon devices as narrow band interference filters, *Instrumentation in Astronomy, SPIE* **28**, 141.

Bonaccini, D. and Smartt, R. N., 1988, Lithium niobate double channel Fabry-Perot interferometer for solar corona uses, *Appl. Optics,* **27**, 5095.

Bray, R., 1988, A computer-controlled triple-Fabry-Perot universal filter for solar research, *LEST Tech. Rept. No. 35.*

Fabry, Ch. and Perot, A., 1898, Sur une spectroscopie interférentielle, *Compt. Rend.* **126**, 331.

Rust, D. M., Appourchaux, T., and Hill, F., 1988, in *Advances in Helio- and Asteroseismology,* J. Christensen-Dalsgaard and S. Frandsen (eds.), D. Reidel, Dordrecht, p. 475.

Rust, D. M. and O'Byrne, J. W., 1991, Vector magnetography, in *Solar Polarimetry,* L. November (ed.), National Solar Observatory, p. 74.

Rust, D. M., Burton, C. H., and Leistner, A. J., 1986, A solid tunable Fabry-Perot etalon for solar seismology, *Instrumentation in Astronomy VI, SPIE* **627**, 39.

Smartt, R. N., 1982, Solar corona photoelectric photometer using mica etalons, *Instrumentation in Astronomy IV, SPIE* **331**, 442.

Vaughan, J. M., 1989, *The Fabry-Perot Interferometer: History, Theory, Practice and Applications*, Adam Hilger, Philadelphia.